FORECASTER'S FORUM

An Unusually Strong Gravity Wave over Western Washington

BRUCE H. BAUCK

NOAA, National Weather Service, Pendleton, Oregon

30 June 1991 and 3 February 1992

ABSTRACT

A mesoscale wave disturbance, observed over western Washington State, is studied through local observations and recognized by comparisons with theory as a large-amplitude gravity wave. It is shown that this gravity wave propagated over 200 km in an atmosphere conducive to wave trapping. Abrupt wind shifts, strong gusty winds to 17 m s^{-1}, moderate-to-severe turbulence, and a sea level pressure fall/rise couplet of 3 to 6 mb were observed as the wave propagated at an average speed of 13 m s^{-1} over the Puget Sound. Subsidence at the top of the marine boundary layer, associated with the trough passage, is estimated at 1100 m over a period of 30 min. This dramatic sinking motion generated rapid, short-lived changes in cloud heights and ceilings, which proved difficult to forecast and potentially dangerous to aviation traffic. A convective downdraft appears to have provided the necessary push to initiate this gravity wave. However, geostrophic adjustment and wind shear cannot be ruled out as possible generation mechanisms.

1. Introduction

On the morning of 7 September 1990, an unusually strong mesoscale event that consisted of rapidly changing cloud distributions and large pressure perturbations moved across much of western Washington State. The rapidly changing winds, cloud ceilings, and surface pressures, combined with the high static stability in the lower atmosphere and the persistence of the mesoscale wave disturbance, suggested it to be a gravity wave. Throughout the following sections, this unusually strong event and its impact on operational forecasts will be described in greater detail.

2. Data

Through the early part of the event, the mesoscale feature was observed concurrently with a line of thunderstorms that was identifiable by radar and some local observations. These thunderstorms formed near Portland (PDX), Oregon, around 1200 UTC and then moved north to Toledo (TDO) in southwest Washington 50 min later. (Refer to Fig. 1 for locations of all referenced sites.) Somewhere over southwest Washington, probably between TDO and Olympia (OLM), this mesoscale wave was initiated. Unfortunately, TDO was the only surface reporting station between PDX and OLM, leaving a huge observation gap. The mesoscale wave quickly moved north past OLM (the first station to report strong winds and rapid pressure changes) and to Seattle before dissipating over northwest Washington.

The propagation speed of the mesoscale disturbance was reasonably constant at 13 m s^{-1} as the disturbance propagated north. The observed period (time interval between successive surface pressure ridges at a fixed point) ranged between approximately 2 h at OLM to 1.5 h at Seattle's International Airport (SEA). These variations may be, in part, attributed to local topographical effects. OLM's closer proximity to the generation point may also account for some of the differences in the period.

The pressure perturbation was one of the most impressive features of this wave event. OLM noted a pressure fall of 5.0 mb in about 20 min (Fig. 2a). The wave seemed to strengthen slightly by the time it reached SEA, where the amplitude increased to 6.1 mb (Fig. 2b). Minor pressure falls and rises on the order of 1 to 2 mb were also observed before and after the major trough passage at SEA. By the time the sea level pressure had stabilized to the apparent background value, the entire event at SEA had lasted around 6 h. Elsewhere across Puget Sound (OLM to PAE), similar pressure signatures were observed.

Local effects on the weather during wave passage were also dramatic. Initially, average surface winds were from the south at 1 to 3 m s^{-1} (3 to 7 kt). Yet with the approach of the deep surface pressure trough at OLM, winds shifted and gusted out of the east-northeast at 11 m s^{-1} (22 kt) (refer to Fig. 3 for sustained surface wind speeds at SEA and OLM). Fifteen minutes later, after passage of the wave trough, winds shifted to southwest and gusted to 17 m s^{-1} (33 kt).

The larger pressure perturbation at SEA resulted in

Corresponding author address: Mr. Bruce Bauck, P.O. Box 668, Pendleton, OR 97801.

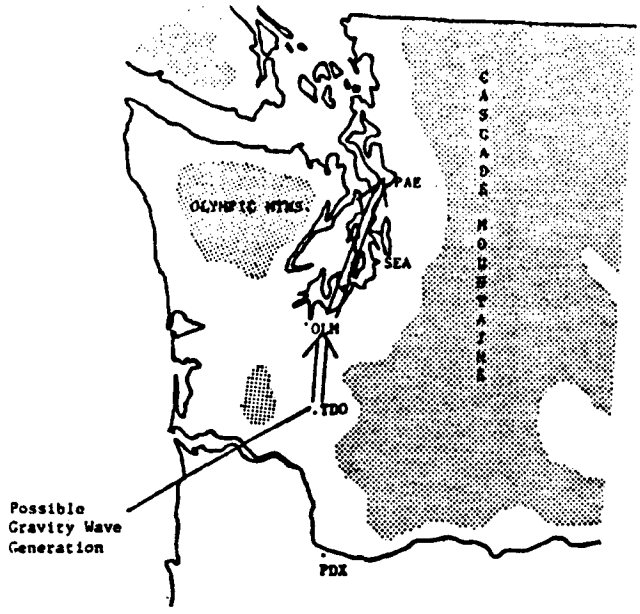

FIG. 1. Map of western Washington, indicating the track of the thunderstorms and the gravity wave.

even greater wind speeds. At 1603 UTC, SEA reported wind gusting out of the northeast at 17.5 m s^{-1} (34 kt). Seven minutes later the wind direction was south with gusts to 15.5 m s^{-1} (30 kt). Farther north, at Everett (PAE), surface wind speeds were less as the gravity wave spread out and weakened. The increase in wind speeds around SEA may be accounted for by the channeling effect of the Olympics to the west and the Cascades to the east.

Obviously, these strong wind speeds, dramatic shifts in wind direction, and rapid changes in aviation weather had a significant impact on operations at local airports. Section 4 provides a discussion of the operational forecast implications associated with the wave event.

The synoptic pattern during the event was dominated by a "vertically stacked" low, from near the surface to 300 mb, centered about 460 km (250 n mi) off the northern California coast. A southerly flow existed over western Washington from 750 mb to above 300 mb. A weak 300-mb jet streak extended from the offshore waters of California, northeast, into Oregon (Fig. 4a). With the position of the upper-level low, a diffluent zone was present over northern Oregon and southern Washington. At 500 mb, advection of cyclonic vorticity by the thermal wind (approximated by thickness lines, Fig. 4b) was associated with a short-wave trough approaching western Oregon. An 850-mb thermal ridge extended from southeast Washington northwestward over western Washington (Fig. 4c). This thermal ridge overlaid a weak, low-level, onshore flow of cool marine air, and resulted in a strong low-level inversion. The top of the inversion was around 830 mb or 1.5 to 2.0 km MSL (5000 to 7000 ft). The atmosphere was very unstable and nearly dry adiabatic above the inversion at Salem (SLE; Fig. 5). An important feature with respect to the more unstable layers aloft was the dryness of the atmosphere just above the inversion, which became increasingly moist with height to near saturation at 550 mb.

3. The 7 September 1990 event: Comparisons to gravity-wave dynamics

A gravity wave is a wave disturbance in which buoyancy acts as the restoring force on parcels displaced from hydrostatic equilibrium. There is a direct oscillatory conversion between potential and kinetic energy in the wave motion. This is analogous to waves produced on a pond when a stone hits the surface. In the case of these shallow-water gravity waves (described by Holton 1979), the restoring force is in the vertical and perpendicular to the direction of movement. Buoyancy waves such as these can be generated by disturbing the surface layer, as with the stone. The horizontal pressure gradient surrounding the depression will cause an inward acceleration. Thus, the fluid will converge horizontally into the depression. This mass convergence must be compensated by horizontal divergence on both sides of the disturbance, resulting in new depressions and so on. These unbalanced horizontal pressure gradients will continue to produce an outward propagation of the wave disturbance. Atmospheric gravity waves propagate in much the same manner. However, the atmosphere has no sharp upper boundary and vertical propagation of energy is possible if no duct or inversion is present. A duct, in this context, is a layer in which strong temperature and moisture gradients act to reflect and transmit or guide wave energy horizontally (Lindzen and Tung 1976).

a. Identification of the 7 September 1990 event

The 7 September mesoscale disturbance has important similarities to previously described atmospheric gravity waves. According to Eom's (1975) linear, two-layer, two-dimensional theoretical model that describes the structure of a simple atmospheric gravity wave, strongest perturbation wind speeds coincide with the high- and low-pressure perturbations. In addition, Schneider (1990), Bosart and Seimon (1988), and Bosart and Sanders (1986) identify gravity waves by abrupt local minima in surface pressure and relative maxima in surface wind speed. A larger disturbance, such as a surface cyclone, would typically have more subtle pressure and wind changes, given the overall weakness of the synoptic pattern on 7 September.

In this particular case, thunderstorms were present, suggesting an outflow boundary as a possible cause for the pressure and wind perturbations. However, the very stable layer present at low levels on the local SLE sounding (Fig. 5) would likely retard any convective downdraft from reaching the surface due to buoyant forces in the cool surface marine layer. If a cool con-

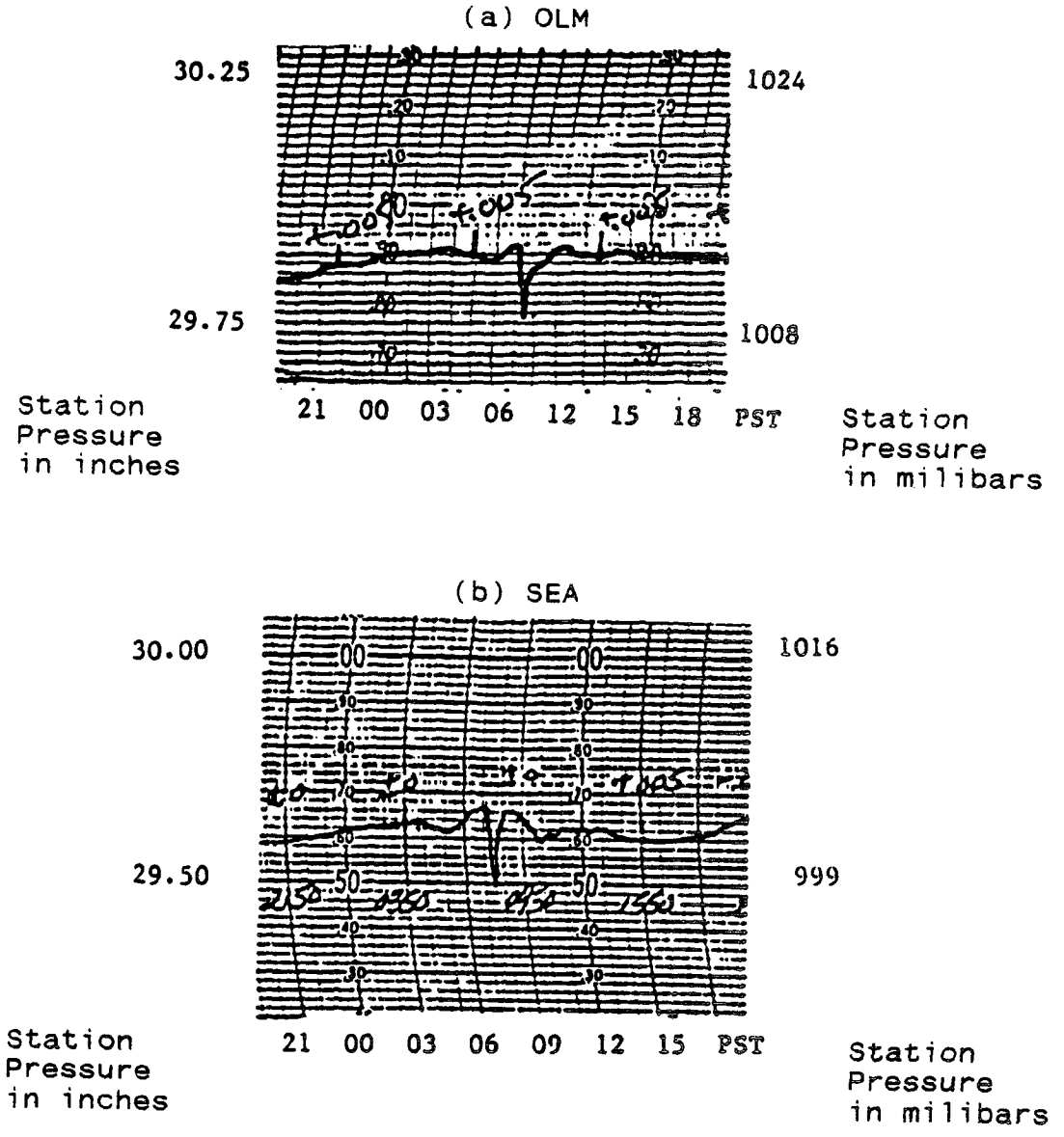

FIG. 2. Pressure traces at OLM (a) and SEA (b), showing passage of the gravity wave.

vective downdraft had penetrated the inversion and reached the surface, temperatures should have warmed dramatically due to adiabatic compression (approximately from 15° to 25°C, according to Fig. 4), when, in fact, no significant surface temperature perturbations were observed with the passage of this mesoscale feature.

Wind and pressure perturbations associated with this event conform with theoretical and observed gravity waves. Thus, evidence strongly suggests this event to be a gravity wave of appreciable magnitude. The generation and maintenance of atmospheric gravity waves will be discussed next, focusing on how they relate to the gravity wave observed over western Washington on 7 September 1990. Emphasis will be placed on the observed environment and similarities to other studied gravity-wave events.

b. Generation processes

Geostrophic adjustment has been hypothesized to play a role in the generation of some gravity waves (Uccellini and Koch 1987; Bosart and Seimon 1988). Geostrophic adjustment may be induced by many different atmospheric processes, although strong upper-level divergence appears to be a common cause. Typically, such a flow configuration is found in the diffluent, exit region of a propagating jet streak as it approaches a downstream ridge. The resulting ageostrophic motion and corresponding mass adjustment

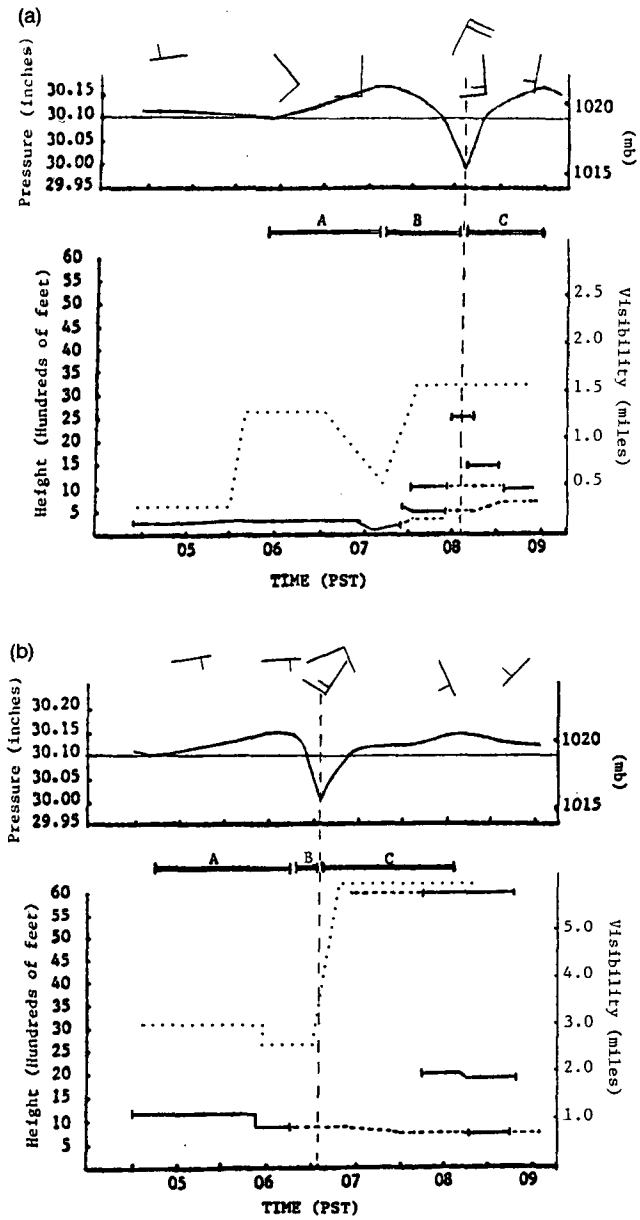

FIG. 3. Pressure trace, wind direction, and speed (top panel), and cloud heights and visibility (bottom panel) at SEA (a) and OLM (b). For cloud heights: dashed lines indicate a scattered layer (a sky cover of 10% to 50%): solid lines indicate cloud heights that are broken or overcast (a sky cover of 60% to 100%). Visibility is represented by the dotted line. Refer to the text for the significance of labeled segments.

forces the atmosphere toward a balanced geostrophic state and releases a substantial amount of energy in some cases (Gossard and Hooke 1975).

With respect to the gravity wave of 7 September, geostrophic adjustment remains a possible production mechanism. At 1200 UTC on the morning of question, an upper-level jet was propagating northeast across northern California into southern Oregon (Fig. 4a). Upper-level diffluence is also apparent across much of Oregon. However, the apparent absence of any features commonly associated with a gravity wave during the first hour of the thunderstorms renders this hypothesis less appealing. For example, PDX and TDO reported no significant pressure or wind changes as the thunderstorms moved by. If geostrophic adjustment were the cause, one would have expected either the gravity wave to form first or the convection and gravity wave to form simultaneously. In this case, the thunderstorms appeared to move a considerable distance before any gravity-wave signature was observed. However, the lack of data across the generation zone (PDX to OLM) will leave enough questions unanswered that the adjustment process cannot be totally ruled out.

A large amount of wind shear at a critical level has also been shown to generate or aid in the development of gravity waves (Stobie et al. 1983). Shear instability gives rise to undulations or small-scale vertical motion. If this motion occurs in a statically stable environment, individual air parcels will undergo buoyancy oscillations similar to what occurs in a gravity wave. For the onset of shear instability, the Richardson number (Ri) should be equal to or less than 0.25. According to Wallace and Hobbs (1977), once turbulence is established within a shear layer, it should be sustained as long as the Richardson number is less than 1. Bosart and Seimon (1988) presented evidence that suggests if the Ri is less than or equal to 0.25, environmental conditions are favorable for gravity-wave generation by shearing instability.

A shear-induced gravity wave is, for the most part, ruled out, since the Richardson number at the critical level was apparently too large (Fig. 5). In addition, local pilot reports indicated only light-to-moderate turbulence at this level. The observed shear appears to have been too weak to produce the strong gravity wave.

The final gravity-wave generation mechanism discussed here is the perturbation of the lower stable layers by convective downdrafts and microbursts. Ferguson (1967) found that deep convection had disturbed a midtropospheric inversion and generated a mesoscale wave disturbance. Convection has also been attributed as a source of wave formation by Bosart and Cussen (1973), Einaudi et al. (1987), and Lin and Goff (1988). The low-level inversion observed in this study was strong enough that any convective downdraft may not have reached the surface, because it would have become positively buoyant in the cold lower layers. However, the associated pulse of energy could have perturbed the stable layer and generated an atmospheric gravity wave.

In this case, the amount of energy released from a microburst could generate a fairly intense gravity wave. The local soundings on the morning of 7 September were very unstable aloft and increasingly moist with height. Upper-air soundings such as these are often found in the Rocky Mountains and the desert of the

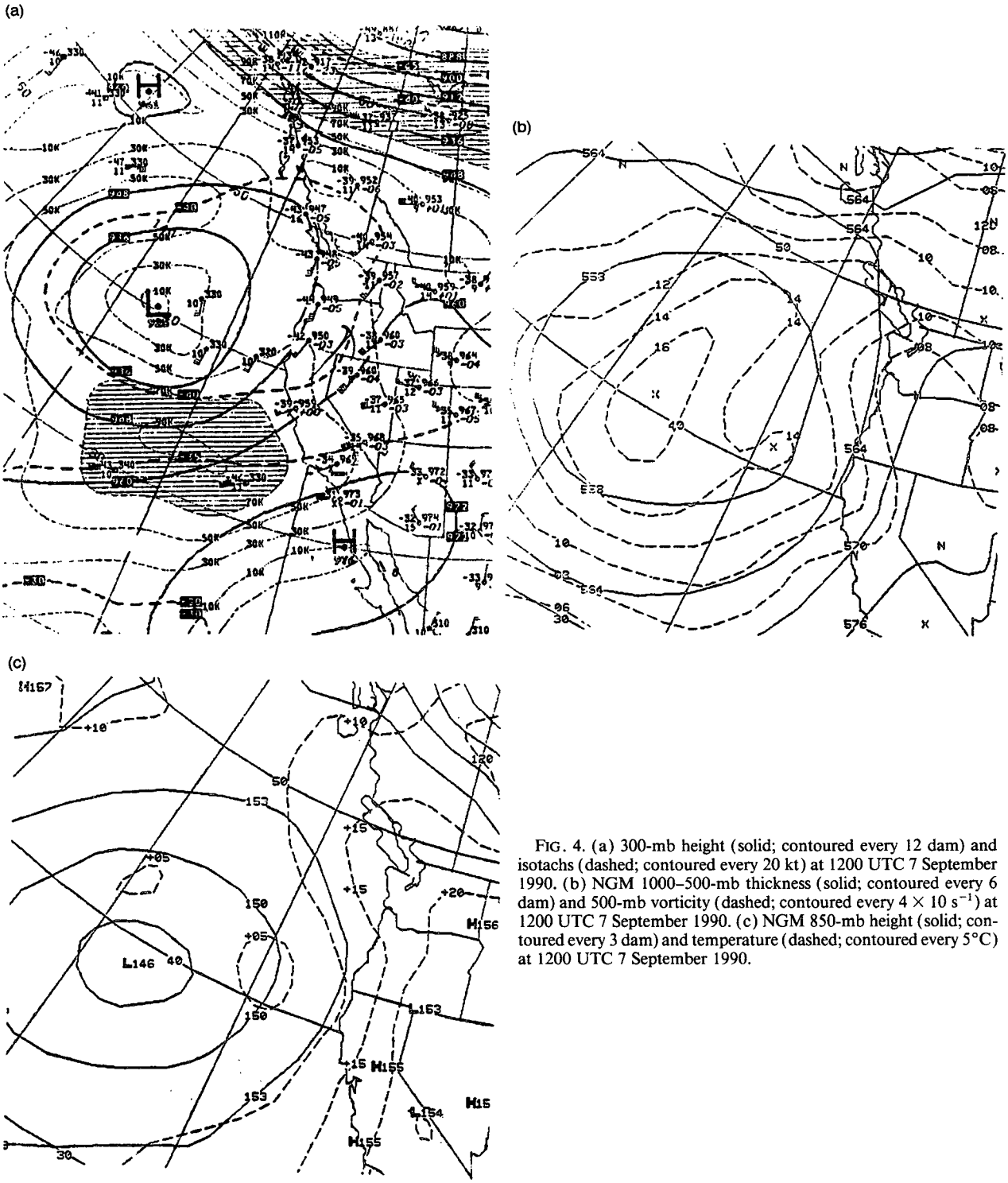

FIG. 4. (a) 300-mb height (solid; contoured every 12 dam) and isotachs (dashed; contoured every 20 kt) at 1200 UTC 7 September 1990. (b) NGM 1000–500-mb thickness (solid; contoured every 6 dam) and 500-mb vorticity (dashed; contoured every $4 \times 10\ s^{-1}$) at 1200 UTC 7 September 1990. (c) NGM 850-mb height (solid; contoured every 3 dam) and temperature (dashed; contoured every 5°C) at 1200 UTC 7 September 1990.

Southwest, and are commonly associated with high-based thunderstorms that produce strong downdrafts and little precipitation due to evaporation. The evaporation cools the downdraft, adding to the negative buoyancy and the overall strength of the downdraft. Wakimoto (1985) discusses conditions considered necessary for an environment to be favorable for dry-microburst activity. Several stations did receive precipitation, but only trace amounts. In fact, as these storms passed by the Weather Service Forecast Office in Seattle, the author observed considerable virga.

According to MacDonald (1976), the upper levels

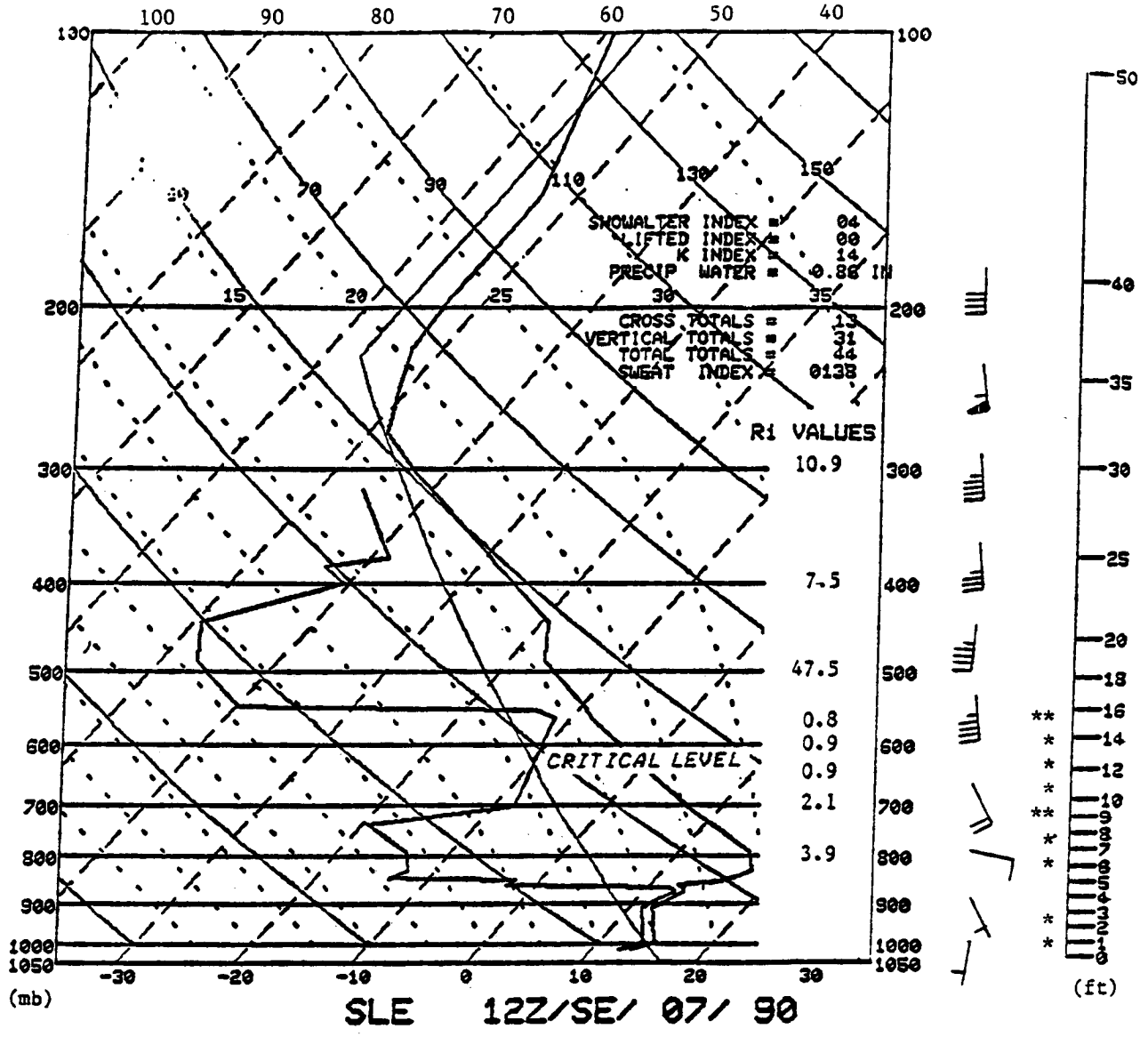

FIG. 5. Salem, Oregon, 1200 UTC sounding. Critical level and selected Richardson numbers (Ri) are also shown. Star symbols (*) plotted vertically to the right of wind direction and speed indicate pilot reports of moderate and severe turbulence from OLM to PAE during the gravity-wave event. Temperature is given in degrees Celsius. The lifted index value is calculated by lifting a parcel, increased by 2°C, from 100 mb above the surface to the lifting condensation level (LCL), and then moist adiabatically to 500 mb, where it is subtracted from the 500-mb temperature (a mean mixing ratio for the lower 100 mb is used in determining the LCL).

(above 3.66 km, or 12 000 ft) must be unstable, and the lower levels dry, for microbursts to take place. Using MacDonald's wind-gust formula and applying it to the SLE sounding, wind gusts above 15 m s^{-1} (30 kt) could have been expected with thunderstorms. Miller (1972) provides another wind-gust formula that yields similar results of 15 to 20 m s^{-1} (30 to 40 kt).

c. Discussion

Thunderstorms, especially those associated with a strong surface inversion, are fairly rare over western Washington. OLM averages only five thunderstorms a year. Gravity waves, especially with the magnitude noted in this case, are also very infrequent. On the other hand, the low-level, marine inversion associated with this overall synoptic pattern is very common. Considering these frequencies and the data already discussed, it is postulated that the approaching, weak, short-wave trough and the upper-level diffluence already in place initiated the thunderstorms but *not* the gravity wave. As the thunderstorms moved north over southwest Washington, a strong downdraft perturbed

the lower stable layer, thereby generating the disturbance. However, after generation, positive feedback from the gravity wave may have helped maintain the thunderstorm complex through the southern Puget Sound. Evidence suggests this interaction, since both features moved northward together.

d. Maintenance criteria

Gravity waves can be maintained in one of two ways: by ducting or trapping the wave energy or by a continual supply of energy (generally from the basic state) to the wave that acts against dissipation. If neither of these mechanisms is present, vertical propagation will quickly disperse the energy from the gravity wave, resulting in dissipation.

With respect to maintenance of the 7 September gravity wave, the important features were the low-level inversion and the unstable characteristics of the atmosphere aloft. As mentioned, a gravity wave with appreciable amplitude and phase speed can propagate without much dissipation through a stable layer or duct. According to Lindzen and Tung (1976), this stable layer should lay below a much deeper, relatively unstable layer that contains a critical level with an Ri of approximately 0.25, where Ri is defined as:

$$\mathrm{Ri} = ((g/T)(\Gamma_d - \Gamma))/(dV/dZ)^2. \qquad (1)$$

The critical level is the level at which the atmospheric flow equals the phase speed of the gravity wave. This configuration will result in considerable wave reflection and enable the wave to propagate over a long distance with little loss of amplitude. Without such a duct, the gravity wave would quickly disperse vertically and decay.

To assess the maintenance mechanism in this case, the important questions are whether or not there was a critical level and what Ri values were present. Knowing that SLE was upstream from the generation area, it is assumed that the SLE upper-air sounding was the most representative. The average direction and propagation speed of north at 13 m s^{-1} (25 kt) for the gravity wave best matches the SLE sounding between 650 and 600 mb. Thus, a critical level exists between these levels. In addition, the average Ri through this same layer was calculated to be 1 or slightly less. In fact, the local minimum Ri (approximately 0.8) is near 570 mb (Fig. 5). In accordance to the Lindzen and Tung (1976) ducting theory, this Ri (0.8) was too large. However, Bosart and Seimon (1988) found that the Ri at the critical level was between 0.5 and 1.0 in some of their cases. In summary, an Ri less than 0.25 optimizes the wave reflectance above the duct, but the implication is that at least a low value of Ri is required.

Bosart and Sanders (1986) presented an expression to calculate the phase speed of a ducted gravity wave (C), assuming ideal conditions, where:

$$C = \frac{2}{\pi}\left[\frac{gH(T_2 - T_1)}{T}\right]^{1/2}. \qquad (2)$$

Here, T_2 and T_1 are the potential temperatures at the top and bottom of the stable layer, respectively; H is the depth of the stable layer; T is the average potential temperature of the stable layer; and g is the gravitational constant.

According to the SLE sounding (Fig. 5), the stable layer existed from the surface to 830 mb. Choosing T_2 = 306.5 K, T_1 = 287.5 K, T = 297 K, and H = 1650 m, C equals 20.5 m s^{-1} for a ducted wave. Given the observed winds below the inversion were south at 1 to 3 m s^{-1} (3 to 7 kt), the wave speed relative to the ground is approximately 18.5 m s^{-1}. As shown previously, the observed wave speed was approximately 13 m s^{-1}.

Several factors may be contributing to the difference between the calculated and observed speeds. Bosart and Sanders (1986) suggested that, for some cases, a reduced Brunt–Väisälä frequency based on moist thermodynamics would be more appropriate than the dry adiabatic value. In the case considered here, the gravity wave existed in a nearly saturated stable layer (Fig. 5). Using Durran and Klemp's (1982) approximated moist Brunt–Väisälä frequency, C reduces to 18.3 m s^{-1}. When low-level environmental winds are taken into account, the wave speed relative to the ground is 16 m s^{-1}. Finally, it may be more suitable to consider the stable layer as being between 830 and 910 mb, since this very stable layer best represents the reflective nature of the duct. In this case, H = 760 m, T_1 = 292.5 K, and with a dry Brunt–Väisälä frequency used, C equals 12 m s^{-1}, which is very close to the observed speed.

e. Subsidence associated with the gravity wave

The large pressure falls at the surface associated with this gravity wave were apparently the result of considerable forced sinking motion. As the major trough of the wave approached, the interface between the relatively cool stable layer and warmer unstable upper layer was displaced rapidly downward, thereby forcing the less-dense air at and above the interface into the lower levels. This displacement produced considerable adiabatic warming and an associated decrease in the surface pressures. The pressure falls continued until the interface reached the minimum elevation in the trough of the gravity wave. Overall, 3- to 6-mb pressure falls were produced by this downward displacement of less-dense air aloft. The hypsometric equation is utilized to estimate the amount of downward motion needed to produce the 6-mb pressure fall observed at SEA:

$$\Delta Z = \frac{RT}{g}\ln\left(\frac{P_b}{P_t}\right), \qquad (3)$$

where ΔZ is the thickness of the atmosphere between the pressure surfaces P_b and P_t; R is the gas constant

for dry air; and T is the mean temperature of the intervening layer.

Simplification dictates the use of only two layers to estimate the amount of sinking motion. However, in reality, many layers existed between the surface and the top of the inversion. One should integrate all these layers to obtain the most accurate estimate of required sinking motion. Figure 6 is a schematic showing a representative skew T–log$p$ sounding with appropriate pressure and temperature symbols.

The first step involves estimating the amount of downward displacement at the interface (ΔZ_2) during the passage of the gravity wave. Once an estimation is established, the hypsometric equation is used to determine the pressure at the displaced interface (represented by P_m on Fig. 6). The initial pressure at the interface is P_t, while P_m is the pressure at the interface after the interface has been forced downward, dry adiabatically, in the base of the gravity-wave trough, and is represented by

$$P_m = P_t \exp\left(\frac{\Delta Z_2 g}{RT_2}\right). \quad (4)$$

Estimating ΔZ_2 to be 1100 m yields a T_2 of 294.5 K, which is the mean temperature of the downward-forced layers. This temperature is fairly high because of adiabatic warming. Using these values yields a P_m of 897.6 mb.

In order to maintain hydrostatic balance, the reduced intermediate pressure (P_m) produces a lower surface pressure. It is now necessary to determine if this value of P_m will result in a surface pressure (P_b) that was approximately what was noted at the SEA airport during the passage of the gravity wave. The hypsometric equation is once again used, but now for the lower layers (from P_m to the surface).

$$P_b = P_m \exp\left(\frac{\Delta Z_1 g}{RT_1}\right) \quad (5)$$

Here, T_1 and ΔZ_1 are the mean temperature and depth of the lower layers. Notice T_1 equals 285.9 K, which is much cooler then the mean temperature of the downward forced layers and is representative of the marine boundary layer. Also, ΔZ_1 equals 1030 m, since the initial depth was 2130 m. This yields a P_b of 1015.2 mb, which agrees with the lowest pressure reported at SEA.

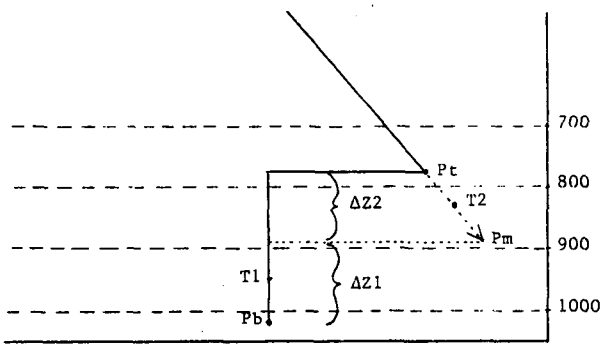

FIG. 6. Schematic showing a representative skew T–log$p$ sounding before and during gravity-wave passage.

In other words, the passage of the gravity wave was associated with approximately 1100 m of forced sinking at and just below the interface in a period of 30 min, which yields a mean vertical velocity of 0.61 m s^{-1}, a result which brings into question the validity of assuming hydrostatic balance. Thus, these results may, at best, be only rough estimates.

4. Operational aspects

This gravity wave had a significant impact on cloud ceilings, visibility, and aircraft operations. As the first crest of the gravity wave approached, and the interface was initially forced upward, the ceiling and visibility lowered at the SEA and OLM airports (Figs. 3a,b; segment A). When the trough of the gravity wave approached each station and forced the interface, and intervening atmospheric layers above each station, downward (Figs. 3a,b; segment B), rapid pressure falls occurred. The rapid sinking motion and resultant adiabatic warming dissipated the low stratus and produced higher visibilities. Bosart and Sanders (1986) remarked that the descent and adiabatic warming in the region of pressure falls should tend to discourage precipitation and dissipate cloud. After trough passage, strong surface convergence and an upward displacement of the interface resulted in rapid surface pressure rises and an increase and lowering of the stratus (Figs. 3a,b; segment C). A shift from IFR to VFR and then back to IFR transpired in less than 45 min at the SEA airport. This brief VFR or MVFR window was common across western Washington as the wave passed.

The impressive changes in wind direction and speed over the brief time span associated with the deep surface pressure trough resulted in considerable turbulence and minor wind damage. Local air traffic noted one of the most serious cases. A Boeing 757 taking off from SEA reported 10-m s^{-1} (20-kt) head winds at 91 m (300 ft) above ground level (AGL). Upon reaching 182 m (600 ft) AGL, and more than likely passing horizontally through the gravity-wave trough, the pilot suddenly experienced a reversal to a 15-m s^{-1} (30-kt) tail wind. According to local reports, the quick action taken by the pilot to increase engine thrust to a maximum possibly saved this aircraft from disaster. Numerous reports of moderate to severe turbulence were also noted as the gravity wave propagated northward across western Washington (refer to Fig. 5 for a vertical plot of local turbulence from OLM–PAE during the gravity wave). Bosart and Seimon (1988) stated that gravity waves are often accompanied by strong vertical wind shear and severe turbulence that pose major hazards to air travel. The strong and abruptly changing winds

were also responsible for numerous downed power lines, a few blown-over trees, and minor structural damage.

The rapid wind shifts associated with this disturbance also had serious implications for airport operations. The switch from light south winds to strong northerlies and then back to strong southerlies at SEA also took only 45 min. For aircraft to maintain maximum lift, different directional runways were required after each wind shift. The rerouting of aircraft to different runways after each wind shift is time consuming and may result in confusion or delays. At SEA, strong north winds lasted less then 15 min. In such situations, airport personnel can be made aware that a wind shift is going to be very brief, and a switch of landing/takeoff patterns may be avoided.

In the case of this gravity wave, the aviation forecaster recognized the type and brevity of the event and responded accordingly. The persistent nature of this event, the static stability of the lower atmosphere, and the overall experience of the local forecaster with such features were key to the real-time recognition. With respect to actual forecasts, such a brief event does not necessarily require amendments to terminal forecasts (FTs), nor is the format of FTs designed to handle such events, especially since conditions were quickly switching from IFR to MVFR and then back. The terminal forecasts already depicted the dominant or overall poor flying conditions. Instead of making time-consuming and possibly misinterpreted updates to the FTs, the anticipated brevity of the event—both in winds and ceiling—were communicated via a phone conversation. This conversation more clearly informed airport personnel of what was to occur and likely produced more decisive airport actions.

5. Conclusion

In the future, when forecasting possible damaging winds, severe turbulence, and/or wind shear associated with high-amplitude gravity-wave events, the pressure perturbation associated with the gravity wave, and the strength of the duct, will be important factors to consider. If a strong low-level inversion and/or a critical level are not present, the gravity wave will probably disperse energy vertically and weaken quickly. On the other hand, ducted gravity waves can maintain their strength and propagate horizontally for possibly hundreds of kilometers (Uccellini and Koch 1987). It is clear from the case presented here that a quickly moving gravity wave, with associated rapid pressure falls and rises, may produce damaging wind and rapid changes in aviation weather. Moderate and possibly severe turbulence may also be observed, especially at the interface or top of the inversion. Such a wave event will continue to pose a serious hazard to local air traffic.

Acknowledgments. Special thanks to Dr. Brad R. Colman, research meteorologist at the WSFO Seattle, for all his help and expertise.

REFERENCES

Bosart, L. F., and J. P. Cussen, Jr., 1973: Gravity wave phenomena accompanying East Coast cyclogenesis. *Mon. Wea. Rev.*, **101**, 446–454.

——, and F. Sanders, 1986: Mesoscale structure in the megalopolitan snowstorm of 11–12 Feb. 1983. Part III: A large-amplitude gravity wave. *J. Atmos. Sci.*, **43**, 924–939.

——, and A. Seimon, 1988: A case study of an unusually intense atmospheric gravity wave. *Mon. Wea. Rev.*, **116**, 1857–1886.

Durran, D. R., and J. B. Klemp, 1982: On the effects of moisture on the Brunt–Väisälä frequency. *J. Atmos. Sci.*, **39**, 2152–2158.

Einaudi, F., W. L. Clark, D. Fua, J. L. Green, and T. E. VanZandt, 1987: Gravity waves and convection in Colorado during July 1983. *J. Atmos. Sci.*, **44**, 1534–1553.

Eom, J. K., 1975: Analysis of the internal gravity wave occurrence of 19 April 1970 in the Midwest. *Mon. Wea. Rev.*, **103**, 217–226.

Ferguson, H. L., 1967: Mathematical and synoptic aspects of a small scale wave disturbance over the lower Great Lakes. *J. Appl. Meteor.*, **6**, 523–529.

Gossard, E. E., and W. H. Hooke, 1975: *Waves in the Atmosphere. Developments in Atmospheric Science, Vol. II.* Elsevier Scientific Publishing Co., 456 pp.

Holton, J. R., 1979: *An Introduction to Dynamic Meteorology.* Academic Press (London), 391 pp.

Lin, Y.-L., and R. C. Goff, 1988: A study of a mesoscale solitary wave originating near a region of deep convection. *J. Atmos. Sci.*, **45**, 194–205.

Lindzen, R. S., and K. K. Tung, 1976: Banded convective activity and ducted gravity waves. *Mon. Wea. Rev.*, **104**, 1602–1617.

MacDonald, A., 1976: Gusty surface winds and high level thunderstorms. Tech. Attachment 76-14, 6 pp. [Available from the Western Region Headquarters of the National Weather Service, Salt Lake City, UT 84147.]

Miller, R. C., 1972: Notes on analysis and severe-storm forecasting procedures of the Air Force Global Weather Central. Tech. Rep. 200 (REV), Air Weather Service, Offutt AFB, NE, 170 pp.

Schneider, S. R., 1990: Large-amplitude mesoscale wave disturbances within the intense midwest extratropical cyclone of 15 December 1987. *Wea. Forecasting*, **5**, 533–558.

Stobie, J. G., Einaudi, F., and Uccellini L. W., 1983: A case study of gravity waves–convective storms interaction: 9 May 1979. *J. Atmos. Sci.*, **40**, 2804–2830.

Uccellini, L. W., and S. E. Koch, 1987: The synoptic setting and possible energy sources for mesoscale wave disturbances. *Mon. Wea. Rev.*, **115**, 721–729.

Wallace, J. M., and P. Hobbs, 1977: *Atmospheric Science: An Introductory Survey.* Academic Press (London), 467 pp.

Wakimoto, R. M., 1985: Forecasting dry microburst activity over the High Plains. *Mon. Wea. Rev.*, **113**, 1131–1143.